Acta Crystallographica Section B
Structural Science
ISSN 0108-7681

Charge-density distribution in hydrogen methylphosphonates of calcium and lithium

Adrian Mermer* and Przemysław Starynowicz*

Wydział Chemii Uniwersytetu Wrocławskiego, ul. F. Joliot-Curie 14, Wrocław 50-383, Poland

Correspondence e-mail: adrian.mermer@gmail.com, przemyslaw.starynowicz@mail.chem.uni.wroc.pl

Received 21 March 2011
Accepted 28 July 2011

Two new crystal structures, calcium bis(hydrogen methylphosphonate), $Ca(CH_3PO_3H)_2$, and lithium hydrogen methylphosphonate, $Li(CH_3PO_3H)$, have been obtained, and the experimental and theoretical charge densities, as well as their topological properties, are reported. Both compounds display layered structures. Each hydrogen methylphosphonate anion coordinates three metal cations in the calcium compound and four in the lithium one. Weak polarization of oxygen lone pairs is observed, with lithium showing somewhat stronger polarization strength than calcium. The reported topological properties from the density functional theory (DFT) and X-ray approach are consistent with each other. In both structures the P—O bonds have a significant share of ionic character. The hyperconjugation effects within the phosphonate group are quenched upon coordination of the metal cations.

1. Introduction

Phosphorus, one of the key chemical elements supporting life (Westheimer, 1987) has always attracted the attention of researchers. As a component of nucleic acids, enzymes and intermediates in many metabolic pathways (Savigniac & Iorga, 2003; Murphy, 2004) it is present mostly in organic phosphate form. On the other hand, inorganic phosphates also play an important role in many fields, *e.g.* nonlinear optics (potassium dihydrogen phosphate, KDP) and agriculture.

Phosphonates constitute another important family of phosphorus compounds displaying a wide variety of properties and possible applications. Owing to their intrinsic tendency to form layered structures (Thompson, 1994; Alberti, 1996) they offer many opportunities to tailor the desired solid-state properties. There are many papers reporting phosphonate–based compounds, covering such fields as intercalation (Zhang *et al.*, 1993; Rao & Vidyasagar, 2005), catalysis (Zeng *et al.*, 2006; Gliga *et al.*, 2011), sensing (Melegari *et al.*, 2008) and nonlinear optical materials (Du *et al.*, 2010). Apart from that phosphonates have been known for their biological activity. The presence of the biochemically inert P—C bond has given rise to the use of nucleoside phosphonates as antiviral drugs, with possible application in tumour therapy (De Clercq & Holý, 2005), whereas the affinity towards Ca^{2+} and Mg^{2+} cations (Matczak-Jon & Videnova-Adrabińska, 2005) has led to the development of bisphosphonate drugs used in therapy of such disorders as osteoporosis, Paget's disease and hypercalcaemia (Sparidans *et al.*, 1998).

Therefore, many reports of the crystal structures of various calcium phosphonates have been published so far (Cao *et al.*, 1990; Langley *et al.*, 1996; Stone *et al.*, 2007; Ślepokura & Lis, 2003). Significantly less research has been devoted to lithium phosphonates, as their potential uses have not been developed

much yet. The possible applications include: electrolyte components or electrode materials in lithium batteries (Cheng & Lin, 2006), and usage as precursors for the synthesis of molecular sieves and ionic conductors (Walawalkar *et al.*, 1997).

Based on these reports we have decided to study the electronic nature of phosphonates by means of X-ray charge-density determination combined with DFT calculations. We have chosen relatively simple systems (the methylphosphonates) in order to establish a basis for further studies on the nature of phosphonic and phosphate compounds, as relatively few papers have covered this field. To date the investigated systems include [(2,4-diamino-pyrimidin-1-io)methyl]phosphonate monohydrate, hereinafter abbreviated to HPPM (Slouf *et al.*, 2002), diphosphonic acid (Lyssenko *et al.*, 2002), phosphoric acid (Souhassou *et al.*, 1995), ammonium dihydrogen phosphate (Pérès *et al.*, 1999), sodium dihydrogen phosphate (Ichikawa *et al.*, 1998), L-arginine dihydrogen phosphate (Espinosa *et al.*, 1996), $AlPO_4$ molecular sieve (Aubert *et al.*, 2003), urea–phosphoric acid (1:1) (Rodrigues *et al.*, 2001) and aminomethylphosphonic acid (Janicki & Starynowicz, 2010).

We thus report two new crystal structures – calcium bis(hydrogen methylphosphonate), $Ca(CH_3PO_3H)_2$, and lithium hydrogen methylphosphonate, $Li(CH_3PO_3H)$, together with the analysis of charge-density distribution. By comparing them to other systems found in the literature we hope to provide some insight into the nature of bonding effects in phosphonic compounds.

2. Experimental

2.1. Preparation of crystals

The mother solutions were prepared by dissolving methylphosphonic acid in small amounts of water and then adding stoichiometric amounts of $CaCO_3$ or Li_2CO_3. The crystals of calcium bis(hydrogen methylphosphonate), hereinafter denoted as (I), were obtained by slow evaporation of the mother solution mixed with a small amount of ethanol. Crystals of lithium hydrogen methylphosphonate (II) were grown by slow evaporation of the mother solution. Appropriate crystals, in the form of colourless plates, were selected from the respective solutions.

2.2. Data collection and refinement

In both cases preliminary diffraction experiments were performed in order to examine the quality of the crystals. All measurements were performed on an Xcalibur diffractometer equipped with a Mo anode, a graphite monochromator, an Onyx CCD area detector and an Oxford Cryosystem cooling device. Data collected up to $\sin\theta/\lambda = 1.15$ Å^{-1} at 85 K [32 821 reflections for (I) and 30 520 in the case of (II)] were used for further processing. The crystal structures were solved and refined with *SHELXS* and *SHELXL* (Sheldrick, 2008) and the results indicated that both crystals were suitable for further investigation. Data were corrected for Lorentz, polarization and absorption factors, the latter calculated from crystal habits; the software used was *CrysAlis CCD* (Oxford Diffraction, 2010). The reflections were scaled and merged with *SORTAV* (Blessing, 1987), giving $R_{int} = 0.0177$ in the $\sin\theta/\lambda$ range of 0.0–0.7 Å^{-1}, 0.0292 in the range of 0.7–1.15 Å^{-1} and 0.0203 for $\sin\theta/\lambda$ between 0 and 1.15 Å^{-1} in the case of (I); for (II) the respective values were 0.0220, 0.0362 and 0.0237.

Multipole refinements were performed with *XD* (Volkov *et al.*, 2006) according to the multipole expansion formula given by Hansen & Coppens (1978)

$$\rho_{atom} = \rho_{core}(r) + P_v\kappa^3\rho_{valence}(\kappa r) + \sum_{l=0}^{l=n}\kappa'^3 R_l(\kappa' r)\sum_{m=-l}^{l} P_{lm}d_{lm}(\theta,\varphi) \quad (1)$$

where ρ_{core} and $\rho_{valence}$ are the spherically averaged electron density functions of the core and valence electrons, P_v is the electron population parameter of the valence shell, κ is the contraction/expansion parameter of the valence-shell radial electron density function, κ' and P_{lm} represent the contraction and population parameters of the multipole functions, d_{lm} are the spherical harmonic functions in real form and r, θ, φ are the spherical coordinates.

Refinements were performed against F and up to $\sin\theta/\lambda = 1.15$ Å^{-1}. The parametrization and constraints applied during the calculations were as follows. The C—H bond lengths were reset after each cycle to 1.09 Å (Allen *et al.*, 1987), and to 1.01 Å for the O1—H bond – the average value taken from the DFT calculations for the clusters (see §2.3). Displacement parameters of the heavy atoms were harmonic anisotropic, with the exception of Ca, for which anharmonic terms (the Gram–Charlier expansion) up to the fourth order were included in the refinement; the anharmonic corrections were not large but their inclusion helped to reduce the peaks around this atom on the residual density maps. The anisotropic temperature factors of the H atoms were simulated with *SHADE* (Madsen, 2006) and then kept fixed during the refinement. P, O and C atoms were modelled as octupoles, for the C-bonded H atoms the dipoles and the quadrupolar terms along the C—H bonds were refined whereas the O-bonded H atoms were expanded up to full quadrupoles. The metal atoms (Ca or Li) were treated as dipoles. The O atoms were divided into two classes: the hydroxyl O1 atom and the terminal O2 and O3 atoms. For P, C and O1 both κ and κ' were refined, whereas for H and metal atoms they were kept fixed at 1.2 for H and 1.0 for Ca or Li. The κ' parameter for the terminal O atoms would not converge to reasonable values, therefore that obtained by Slouf *et al.* (2002), 0.73, was used. The electroneutrality constraint was applied to the whole asymmetric unit in both cases, thus allowing charge transfer between the ions. The scattering factors calculated from Clementi–Roetti wavefunctions (Clementi & Roetti, 1974) for the core and spherical valence parts of the atomic charge distribution were used. The radial deformation functions $R_l(r)$ were in the form of single Slater functions $[\zeta^{n+3}/(n+2)!]r^n\exp(-\zeta r)$. For phosphorus the n value was set to 6 for all orders of multi-

Table 1
Data collection and refinement details for (I) and (II).

Only reflections with sin $\theta/\lambda \leq 1.15$ Å^{-1} are taken into account. Experiments were carried out at 85 K with Mo $K\alpha$ radiation using an Xcalibur Onyx diffractometer. Refinement was with 0 restraints. H-atom parameters were constrained.

	(I)	(II)
Crystal data		
Chemical formula	$C_2H_8CaO_6P_2$	CH_4LiO_3P
M_r	230.10	101.95
Crystal system, space group	Monoclinic, $C2/c$	Monoclinic, $P2_1/c$
a, b, c (Å)	20.403 (13), 5.601 (2), 7.274 (6)	9.267 (5), 4.604 (2), 9.384 (3)
β (°)	108.48 (8)	96.12 (4)
V (Å^3)	788.4 (9)	398.1 (3)
Z	4	4
μ (mm^{-1})	1.18	0.53
Crystal size (mm)	0.48 × 0.35 × 0.06	0.46 × 0.34 × 0.06
Data collection		
Absorption correction	Analytical *CrysAlis RED* (Oxford Diffraction Ltd, 2010)†	Analytical *CrysAlis RED* (Oxford Diffraction Ltd, 2010)†
T_{min}, T_{max}	0.667, 0.941	0.832, 0.970
No. of measured, independent and observed [$I > 3\sigma(I)$] reflections	32 821, 5010, 4683	30 520, 5066, 4610
R_{int}	0.020	0.024
Refinement		
$R(F)$, $wR(F^2)$, S for $F^2 > 3\sigma(F^2)$: spherical refinement	0.016, 0.047, 2.634	0.021, 0.056, 2.851
$R(F)$, $wR(F^2)$, S for $F^2 > 3\sigma(F^2)$: multipole refinement	0.012, 0.026, 1.455	0.016, 0.031, 1.470
No. of reflections	4683	4610
No. of parameters	174	169
$\Delta\rho_{max}$, $\Delta\rho_{min}$ (e Å^{-3})	0.39, −0.24	0.35, −0.22

† Version 1.171.33.32 (release 27-01-2009 *CrysAlis*171.NET; compiled 27 January 2009). Analytical numeric absorption correction using a multifaceted crystal model based on expressions derived by Clark & Reid (1995).

poles, following Espinosa *et al.* (1996), and the initial ζ value was 5.19 bohr $^{-1}$.

No extinction correction was included, as in both cases the calculated values of the extinction parameter were negative. Attempts to refine other models (*e.g.* with hexadecapoles included for various combinations of atoms and with κ' factors at 1.0 for C and O atoms) led to less encouraging results, which was especially noticeable when the Bader charges were analyzed. It was eventually found that κ' for the terminal O atoms must be reduced if the Bader charges at least approximately consistent with the theoretical values were to be obtained.

A Hirshfeld (Hirshfeld, 1976) rigid-bond test was performed in each case showing satisfactory results; the highest values occurring for the C—P bond and being 1.2 × 10^{-3} Å^2 for (I) and 1.1 × 10^{-3} Å^2 for (II). The crystal data and refinement details for both crystals are presented in Table 1.[1]

[1] Supplementary data for this paper are available from the IUCr electronic archives (Reference: SO5049). Services for accessing these data are described at the back of the journal.

For comparison purposes we have performed spherical refinements with *XD* on the same set of data as that used for the multipole refinements.

Topological parameters were calculated for the asymmetric part of the unit cell with several atoms added so that the metal cation and the O atoms could be provided with their closest neighbours and the atomic basins were given adequate boundaries.

2.3. Theoretical calculations

The DFT calculations were performed with the *ADF* suite of programs (Baerends *et al.*, 2008). For the calculations the following systems were taken:

(i) free methylphosphonic acid [in two geometries, one taken from (I) and the other from (II); the main difference between them is in the H—O—P—C torsion angle, see §3];

(ii) a cluster of 13 methylphosphonate anions and three calcium cations;

(iii) a cluster of eight methylphosphonate anions and four Li cations.

In cases (ii) and (iii) the clusters were chosen so that one methyl phosphonate anion was provided a full neighbourhood of metal cations, which in turn were supplied with their full coordination environments. For the natural bond orbitals (NBO) analysis (Glendening *et al.*, 2001) small clusters composed of the hydrogen methylphosphonate anion together with three Ca or four Li cations were used. Firstly, the positions of the H atoms were optimized, whereas the positions of non-H atoms were kept fixed as input from the X-ray conventional refinement. Also the H—C—P and H—O—P bond angles and the H—C—P—O and H—O—P—C torsion angles were kept frozen to prevent undesired migrations of the H atoms. When the optimization converged, the charges were computed, and the NBO and topological analyses were performed. The functional PW91 (Perdew *et al.*, 1992), and the basis – TZ2P, composed of double z functions for core electrons, triple z for valence ones and two polarization functions, with unfrozen cores, were used throughout. The NBO analysis of the methylphosphonate anion, together with the calculation of resonance Lewis structures, was performed with *NBO*5.0 (Glendening *et al.*, 2001). The topological analysis of the theoretically calculated electron density was performed with *Xaim* (Ortiz & Bo, 1998). The kinetic energy density, G, at the critical point, $\mathbf{r}_c$, was calculated using the formula (Abramov, 1997)

Table 2
Selected geometrical parameters (Å, °) for (I) and (II).

	(I)	(II)
P—O1	1.5783 (2)	1.5789 (2)
P—O2	1.5123 (2)	1.5070 (2)
P—O3	1.5163 (2)	1.5213 (2)
P—C	1.7896 (2)	1.7866 (2)
O1—P—O2	106.83 (2)	109.80 (2)
O1—P—O3	111.96 (2)	108.44 (2)
O2—P—O3	114.39 (1)	113.62 (1)
O1—P—C	102.30 (2)	105.29 (2)
O2—P—C	110.17 (2)	110.83 (2)
O3—P—C	110.48 (1)	108.50 (2)

Hydrogen bond and M—O distances for (I)

	D—H (Å)	H···A (Å)	D···A (Å)	D—H···A (°)
O1—H1···O3^{i}	1.01	1.63	2.6290 (3)	171

Ca—O distances (Å)

Ca—O2^{ii}	2.3841 (2)	Ca—O2	2.4043 (2)
Ca—O3^{iii}	2.3740 (2)	Ca—O(1)	3.0110 (3)

Symmetry code(s): (i) $x, -y, z+\frac{1}{2}$; (ii) $1-x, 1-y, 1-z$; (iii) $x, y+1, z$.

Hydrogen bond and M—O distances for (II)

	D—H (Å)	H···A (Å)	D···A (Å)	D—H···A (°)
O1—H1···O3^{i}	1.01	1.67	2.6433 (3)	162

Li—O distances (Å)

Li—O2	1.9087 (5)	Li—O3^{iii}	1.9717 (6)
Li—O2^{ii}	1.9278 (5)	Li—O3^{iv}	2.0406 (5)

Symmetry codes: (i) $x, y-1, z$; (ii) $-x+1, y+\frac{1}{2}, \frac{3}{2}-z$; (iii) $x, -y+\frac{1}{2}, z-\frac{1}{2}$; (iv) $-x+1, y-\frac{1}{2}, \frac{3}{2}-z$.

$$G(\mathbf{r}_c) = 3/10(3\pi^2)^{2/3}\rho(\mathbf{r}_c)^{5/3} + 1/6\nabla^2\rho(\mathbf{r}_c), \quad (2)$$

and the local virial theorem (Bader, 1994) was applied to obtain the potential energy density, V

$$V(\mathbf{r}_c) = 1/4\nabla^2\rho(\mathbf{r}_c) - 2G(\mathbf{r}_c). \quad (3)$$

3. Results and discussion

3.1. Crystal structures

Both crystals are built up from hydrogen methylphosphonate anions and the metal cations. The anions in (I) and (II) have essentially the same geometry (Table 2), although some subtle differences may be found when certain geometrical parameters are examined.

First the orientation of the hydroxyl H atom in (I) is different from that in (II), as the bond angles H—O—P [121° in (I) and 103° in (II)] and the torsion angles H—O—P—C [138 and −106° in (I) and (II)] show.

Second the bond lengths of O2—P and O3—P in (I) are very similar, whereas in (II) they differ slightly. In both structures, however, the bonds formed by the hydroxyl oxygen O1 with P are longer than those formed by the other O atoms. Apart from that slight differences of the respective O—P—C and O—P—O angles may be observed, *cf.* Table 2.

All bond lengths are consistent with those found in the literature (Walawalkar *et al.*, 1997; Cao *et al.*, 1990; Zhang & Clearfield, 1992). Both compounds display a layered crystal structure found in many metal-organic phosphonate networks (Thompson, 1994; Alberti, 1996), where the organic parts of the anions face each other, thus forming separate layers, often of hydrophobic nature. This is also the case for (I) and (II). In both structures the anions lie above and below the surface formed by Ca or Li cations, with the methyl groups pointing outwards. The polymeric layers are perpendicular to **a*** in both structures (see Fig. S1 in supplementary material).

In (I) the anion bonds to three calcium cations (Fig. 1), whereas each calcium cation (which is located on a twofold axis) coordinates to six O atoms (O2 and O3 and their symmetry generated offsprings, see Table 2) which form the first coordination sphere; apart from that two hydroxyl O1 atoms are *ca* 3 Å away. The calcium cations are connected *via* two μ-bridging O2 atoms along the **c** axis, thus forming infinite zigzag chains composed of four-membered Ca_2O_2 rings with the Ca cations shared. The chains in turn are connected through O3—P—O2 bridges along the **b** direction. The O1 hydroxyl O atom is involved in a hydrogen bond with O3. In (II) the anion forms bonds to four Li cations (Fig. 2); the latter are four-coordinate. The coordination figure is spanned by two O2 and two O3 atoms, assuming the shape of a distorted tetrahedron. Both O2 and O3 are involved in μ_2 bridges with two adjacent Li cations, thus giving rise to a complex system of four-, six- and eight-membered rings and consequently to the formation of a two-dimensional metal-organic framework. The remaining O1 atoms are donors in hydrogen bonds formed with O3 atoms. The hydrogen and metal–oxygen bonds for both structures are presented in Table 2.

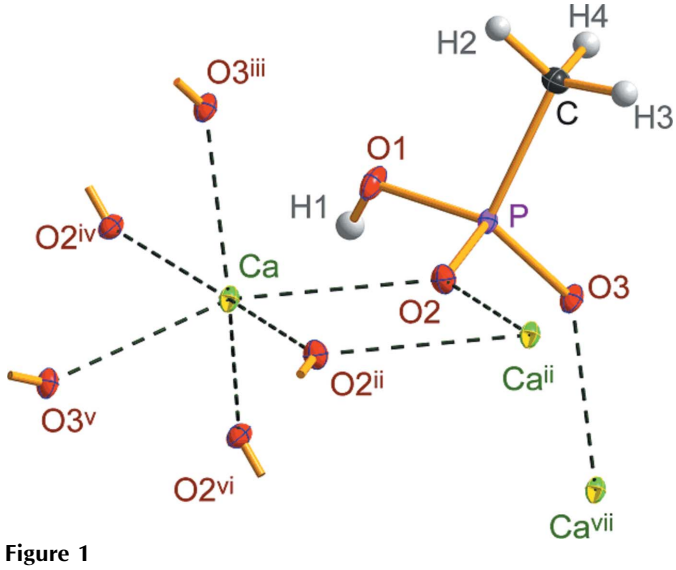

Figure 1
Coordination of the hydrogen methylphosphonate anion and calcium cation in (I). The symmetry operators are taken from Table 2 plus: (iv) $x, 1-y, \frac{1}{2}+z$; (v) $1-x, 1+y, \frac{3}{2}-z$; (vi) $1-x, y, \frac{3}{2}-z$; (vii) $x, -1+y, z$.

Table 3
Experimental and theoretical Bader (Q_B) and Hirshfeld (Q_H) charges for both compounds.

The theoretical charges labelled as Q refer to clusters (ii) and (iii) (see §3.5), those marked as Q' represent the quantities calculated for isolated $CH_3PO_3H^-$ *in vacuo*.

	Multipole refinement		DFT calculations			
	Q_B	Q_H	Q_B	Q_H	Q'_B	Q'_H
(I)						
Ca	1.74	0.36	1.65	0.33 (0.30–0.32)†		
P	3.52	0.26	3.43 (3.41–3.47)	0.48 (0.35–0.44)	3.41	0.28
O1	−1.38	−0.19	−1.43 (−1.36 to −1.45)	−0.21 (−0.20 to −0.28)	−1.37	−0.27
O2	−1.47	−0.22	−1.51 (−1.47 to −1.52)	−0.28 (−0.28 to −0.46)	−1.52	−0.52
O3	−1.57	−0.27	−1.51 (−1.47 to −1.54)	−0.27 (−0.28 to −0.52)	−1.54	−0.51
C	−0.85	−0.17	−0.50 (−0.49 to −0.52)	−0.18 (−0.18 to −0.20)	−0.47	−0.19
H1	0.64	0.19	0.65 (0.54–0.65)	0.11 (0.08–0.16)	0.56	0.14
H2	0.11	0.11	0.01 (−0.06–0.03)	0.03 (−0.02–0.03)	−0.03	0.01
H3	0.08	0.05	0.05 (−0.07–0.05)	0.03 (0.00–0.04)	−0.03	0.02
H4	0.10	0.06	−0.05 (−0.09 to −0.06)	0.01 (−0.02–0.00)	−0.01	0.03
$CH_3PO_3H^-$	−0.62	−0.18	−0.86	−0.28		
(II)						
Li	0.91	0.23	0.91 (0.90–0.91)	0.16 (0.15–0.16)		
P	3.63	0.42	3.41 (3.38–3.46)	0.49 (0.34–0.42)	3.45	0.29
O1	−1.50	−0.30	−1.39 (−1.35 to −1.41)	−0.22 (−0.20 to −0.29)	−1.35	−0.27
O2	−1.52	−0.25	−1.56 (−1.47–1.57)	−0.32 (−0.34–0.46)	−1.52	−0.52
O3	−1.71	−0.29	−1.52 (−1.47 to −1.53)	−0.28 (−0.28 to −0.51)	−1.52	−0.51
C	−0.93	−0.19	−0.50 (−0.48 to −0.50)	−0.17 (−0.17 to −0.20)	−0.54	−0.18
H1	0.67	0.19	0.61 (0.55–0.61)	0.10 (0.09–0.15)	0.56	0.13
H2	−0.10	0.08	−0.03 (−0.07 to −0.02)	0.02 (−0.01–0.02)	−0.03	0.01
H3	0.19	0.07	0.07 (−0.04–0.10)	0.05 (0.01–0.06)	0.00	0.03
H4	0.08	0.05	−0.03 (−0.07 to −0.02)	0.02 (−0.01–0.02)	−0.02	0.02
$CH_3PO_3H^-$	−1.19	−0.22	−0.94	−0.31		

† The first value represents the atom belonging to the central molecule provided with all O–metal and hydrogen bonds; the values in parentheses show the range obtained for respective atoms in the peripheral molecules.

3.2. Residual maps

The residual maps from the multipole refinements for (I) and (II) (Fig. S2 in the supplementary material) generally show satisfactory levels of unaccounted charge density. In (I) the highest peak (0.39 e Å^{-3}) is located 1.86 Å away from O3. The highest peak near Ca (0.55 Å away) has 0.31 e Å^{-3}, whereas the deepest hole near Ca (0.52 Å away) reaches −0.23 e Å^{-3}. The highest peak in the neighbourhood of P (0.83 Å away) is located on the P—O1 bond and has 0.26 e Å^{-3}; the deepest hole (0.46 Å away from P) has −0.24 e Å^{-3}. In (II) the highest peak (0.35 e Å^{-3}) is 0.80 Å from H1, and the deepest hole (−0.22 e Å^{-3}) is 0.91 Å away from P.

3.3. Atomic charges

The atomic charges computed from the experimental electron-density distribution and from the theoretical calculations are presented in Table 3. There are three types of charges that may be obtained from the experimentally determined charge distribution – monopole populations (Q_{mp}), Bader charges (Q_B; Bader, 1994) and Hirshfeld charges (Q_H; Hirshfeld, 1977). Of these the monopole populations do not have (in this paper) their theoretically computed counterparts; their values, together with contraction parameters, are given in the supplementary materials, Table S1.

The experimental Bader and Hirshfeld charges are comparable with the theoretical values, although the match is not always perfect. The metal charges are in quite good agreement, especially in the case of Ca. In (I) the charges of P and O atoms agree well, while in (II) the experimentally derived Bader charges exceed those obtained from the DFT calculations. The O3 atom especially shows more negative charge, −1.71 e, which is ∼0.19 e lower than the expected value. Also, the charges of O1 are lower (0.11 and 0.08 e in the case of the Bader and Hirshfeld charges). The absolute values of the experimental Bader charges of the C atom are higher in both structures. In the DFT case the charges of C atoms are *ca* −0.5 e, whereas in the experimental case they adopt values close to −0.9 e. These highly negative values may be a side effect of including fixed anisotropic displacement parameters for H atoms. The experimental Bader and Hirshfeld charges resemble those reported for aminophosphonic acid [where the respective Bader/Hirshfeld charges were: P = 3.41/0.19, O(H) = −1.31/−0.21, O(terminal) = −1.41 and −1.52/−0.45 and −0.48, C = −0.29/−0.08], although in (I) their absolute values are slightly lower and in (II) higher. These differences may in a

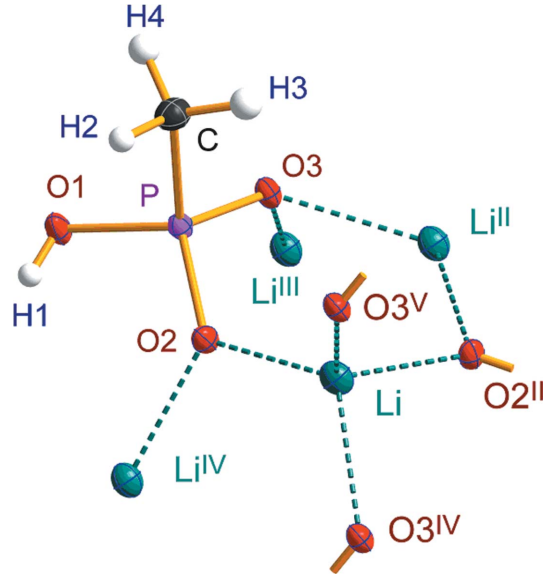

Figure 2
Coordination of the hydrogen methylphosphonate anion and lithium cation in (II). The symmetry operators are taken from Table 2 plus: (v) $x, \frac{1}{2}-y, -\frac{1}{2}+z$.

Table 4
Selected topological parameters for (I) and (II).

	Experimental				Theoretical†		
	ρ (e Å^{-3})	$\Delta\rho_c$‡ (e Å^{-3})	$\nabla^2\rho_c$ (e Å^{-5})	ε	ρ_c (e Å^{-3})	$\nabla^2\rho_c$ (e Å^{-5})	ε
(I)							
P—O1	1.316 (9)	0.176	14.68 (4)	0.10	1.334 (1.282)	16.31 (17.26)	0.08 (0.09)
P—O2	1.569 (11)	0.301	20.60 (4)	0.05	1.547 (1.557)	24.51 (24.65)	0.03 (0.04)
P—O3	1.520 (11)	0.265	19.92 (4)	0.05	1.526 (1.542)	21.98 (22.02)	0.17 (20)
O1—H1	2.29 (6)	0.70	−43.7 (4)	0.04	2.00 (2.07)	−45.35 (−39.18)	0.01 (0.02)
P—C	1.202 (9)	0.279	−3.67 (3)	0.09	1.217 (1.192)	−8.75 (−7.69)	0.00 (0.03)
C—H2	1.84 (5)	0.61	−20.5 (2)	0.03	1.84 (1.83)	−23.77 (−23.24)	0.04 (0.05)
C—H3	1.80 (5)	0.53	−18.3 (2)	0.00	1.85 (1.83)	−23.54 (−22.61)	0.02 (0.03)
C—H4	1.81 (6)	0.60	−18.8 (3)	0.02	1.82 (1.82)	−21.94 (−22.41)	0.02 (0.02)
O2—Ca	0.180 (3)	−0.018	4.030 (1)	0.07	0.226	3.84	0.03
O2—Ca^{i}	0.208 (1)	0.004	4.194 (1)	0.05	0.228	4.04	0.02
O3—Ca^{ii}	0.219 (2)	0.014	4.252 (1)	0.03	0.230	4.17	0.04
H1—O3^{ii}	0.44 (4)	0.016	0.04 (8)	0.14	0.39	2.48	0.01
(II)							
P—O1	1.321 (7)	0.177	15.01 (3)	0.05	1.346 (1.306)	15.93 (16.68)	0.14 (0.12)
P—O2	1.566 (8)	0.282	24.53 (3)	0.06	1.561 (1.568)	25.69 (26.00)	0.01 (0.02)
P—O3	1.539 (8)	0.289	21.99 (3)	0.03	1.517 (1.531)	22.69 (23.11)	0.04 (0.02)
O1—H1	2.15 (5)	0.59	−40.9 (4)	0.09	2.08 (2.39)	−46.20 (−53.47)	0.01 (0.02)
P—C	1.201 (8)	0.266	−2.32 (3)	0.05	1.219 (1.188)	−8.38 (−6.54)	0.00 (0.02)
C—H2	1.83 (7)	0.59	−17.1 (3)	0.01	1.81 (1.80)	−22.20 (−21.49)	0.03 (0.02)
C—H3	1.78 (7)	0.55	−17.8 (3)	0.02	1.85 (1.81)	−23.55 (−22.00)	0.03 (0.02)
C—H4	1.84 (6)	0.59	−18.2 (3)	0.02	1.82 (1.80)	−22.24 (−21.42)	0.02 (0.01)
O2—Li	0.187 (6)	0.017	5.589 (4)	0.05	0.212	5.15	0.01
O2—Li^{iii}	0.162 (5)	0.002	5.273 (4)	0.06	0.203	4.88	0.01
O3—Li^{iv}	0.114 (6)	−0.009	3.595 (4)	0.07	0.151	3.52	0.05
O3—Li^{v}	0.172 (7)	0.029	4.434 (5)	0.03	0.177	4.26	0.04
H1—O3^{vi}	0.29 (3)	−0.10	3.75 (8)	0.24	0.35	2.71	0.02

Symmetry codes: (i) $-x+1, -y+1, -z+1$; (ii) $x, y-1, z$; (iii) $-x+1, y-\frac{1}{2}, -z+\frac{3}{2}$; (iv) $-x+1, y+\frac{1}{2}, -z+\frac{3}{2}$; (v) $x, -y+\frac{1}{2}, z+\frac{1}{2}$; (vi) $x, y-1, z$. † The values retrieved from the cluster calculations are given first and values for isolated anions are given in parentheses. ‡ Deformation density at the critical point.

3.4. Topological parameters, bond degrees and local energy densities

Examination of the topological properties (Table 4) discloses satisfactory similarity of the experimentally obtained ρ_c (electron density at the bond critical point, BCP) and $\nabla^2\rho_c$ (Laplacian of the former), and those obtained from DFT calculations for clusters (ii) and (iii), see §2.3.

The ρ_c values for P—O bonds in (I) retrieved from experiment are in good agreement with analogous values for (II). As has been observed previously (Slouf *et al.*, 2002; Janicki & Starynowicz, 2010), the density at the critical point of the P—O(H) bonds is lower compared with P–O(unprotonated) bonds. The DFT values are located close to the respective experimental values. The experimental $\nabla^2\rho$ show satisfactory agreement with the theoretical ones, but are slightly lower for (I). Rather high (positive) values of the Laplacians suggest considerable ionicity of the bonds – greater in the case of those involving unprotonated O atoms. This can be explained by a greater concentration of negative charge on these atoms, as discussed earlier. On the whole the results correspond well with the previous studies on HPPM or aminomethylphosphonic acid. Slouf *et al.* (2002) report BCP densities that are very similar to ours, but generally slightly lower – 1.28 e Å^{-3} for the P—O(H) bond and 1.49–1.50 e Å^{-3} for the P—O bonds, whereas their $\nabla^2\rho$ values are 20–40% higher. The values of ρ_c and the Laplacian obtained by Janicki & Starynowicz are almost identical to ours (save ρ_c for one unprotonated atom), which largely results from similar approaches in the refinement procedure adopted in the quoted study and in the present paper. On the other hand, comparing the values given by Aubert *et al.* (2003) and Espinosa *et al.* (1996) for the phosphate groups [1.55–1.68 e Å^{-3} for P—O bonds and 1.46 e Å^{-3} for P—O(H) bonds] it can be observed that phosphate P—O bonds have somewhat larger values of ρ_c.

The P—C bond shows satisfactory agreement of theoretical and experimental results in terms of ρ_c, but not of the Laplacian. The former quantity is slightly larger than in aminophosphonic acid [1.167 (7) e Å^{-3}] or in HPPM (1.09 e Å^{-3}), whilst the Laplacians are *ca* 5–6 e Å^{-5} larger than the DFT values, but on the other hand they are closer to those reported by Slouf *et al.* (2002).

The parameters of the unique O—H···O′ bonds locate these interactions in the strong hydrogen bond (HB) area. The way reflect the difference between the polarizing power of Ca^{2+} and Li^{+}, although in view of the theoretical calculations these differences may seem overestimated. It may also be noticed that the theoretical charges of a few atoms from the anion *in vacuo* (Q'_B and Q'_H) are different from those calculated for the cluster. This concerns mainly the Hirshfeld charges of the terminal O and P atoms; for other atoms the changes are minor. Somewhat surprisingly, the growth of the positive Hirshfeld charge of P together with the increase of the negative ones for O2 and O3 is not reflected in the values of the Bader charges. This, together with small Hirshfeld charges of the metal cations, may indicate that the Q_H parameter is very sensitive to coordination, contrary to the rather insensitive Bader charge. As noticed earlier for aminomethylphosphonic acid, the hydroxyl O atoms (labeled O1) show lower Bader charges than the non-hydroxyl ones. The anomalously negative Bader charge of O3 in (II) is probably an artifact. Also, the experimental Hirshfeld charge of O1 is lower than the theoretical one; this is probably because of the imperfect separation of anisotropic vibrations from the quadrupolar deformation in the case of the H1 atom. Both the experimental and theoretical Bader and Hirshfeld charges of C are more negative than in the $NH_3CH_2PO_3H$ molecule.

approximate hydrogen-bond energies, calculated using the formula given by Espinosa *et al.* (1998)

$$E_{HB} = \frac{1}{2}V(r_c) \quad (4)$$

for the experimental and DFT approaches, are 80.1 and 74.8 kJ mol^{-1} for (I), and 57.8 and 65.6 kJ mol^{-1} for (II). This is additionally supported by the relatively high Hessian matrix eigenvalues λ_1, λ_2 and λ_3 (Table S2 in the supplementary materials) which indicate a tightening of ρ in the hydrogen-bond BCP area, characteristic for strong interactions (Espinosa, Souhassou *et al.*, 1999; Espinosa, Lecomte & Molins, 1999).

The parameters of the Ca—O and Li—O bonds resemble those of weak hydrogen bonds. The charge density at the Ca—O BCP is slightly higher than that reported for the Sr—O bond in cubic $SrTiO_3$ [0.10 (2) e Å^{-3} reported by Zhurova & Tsirelson (2002) or 0.18 (1) e Å^{-3} reported by Jauch & Reehuis (2005)]. Also the Laplacians for the present Ca—O bonds are higher [4.030 (1)–4.252 (1) e Å^{-5}] than for the Sr—O bonds [2.40 (3) and 2.27 (2) e Å^{-5}]. The ρ_c values of the Li—O bonds are up to 0.07 e Å^{-3} larger than the density reported for the Li—O bond in $Li[N(CH_3)_4]_2[Co(NO_2)_6]$ (Bianchi *et al.*, 1996), also the Laplacians are slightly higher for the present compounds. This is probably in a great part brought about by the longer Li—O distance [2.0299 (2) Å] in the crystal of the cobalt complex. The values of ρ_c for the Li—O bonds are two to three times greater on average than those for K–O bonds in $KMnO_4$ (0.077 e Å^{-3}) or in $KClO_4$ (0.065 e Å^{-3}; Marabello *et al.*, 2004); the same holds for the values of the Laplacians: for Li—O they are 3.595 (4)–5.589 (4) e Å^{-5}, while for K—O they are 0.98 (2)–1.74 (3) e Å^{-5}.

In order to check if the densities at the critical points of these bonds result only from mere overlapping of the peripheral atomic electron densities or whether some polarization and/or covalent effects are active, we have calculated, following the ideas set out by Aubert *et al.* (2003), the deformation charge density at the critical points $\Delta\rho_c$. The values of $\Delta\rho_c$ are given in Table 4. Their inspection reveals that in the case of the Ca—O bonds they oscillate near 0. On the other hand there is a small positive excess for all, except the longest one, Li—O bonds – its contribution to the total density at the BCPs ranges up to 17% (compared with 6% of the maximum share in the case of Ca—O bonds). In this way the difference between the soft calcium cation and the hard, strongly polarizing Li^+ may be observed. The influx of electron density in the critical point is the result of polarization of a lone pair of adjacent O atoms, as illustrated in Fig. 3. The experimental deformation densities calculated along the *M*—O lines shown in Fig. 4 confirm that the charge accumulates to a greater degree between Li and O atoms than between Ca and O ones. This holds true for all the Li—O bonds except the longest one – the O3—Li^{iv} bond. It is noteworthy that O3 in (II) is additionally an acceptor of a strong hydrogen bond, which directs the main part of the deformation density towards it. This leaves the coordinating lithium cation somewhat aside and consequently a deficit of electron density in this region can be observed.

It may also be observed that $\Delta\rho_c$ values for the P—C and P—O1 bonds are comparable to those reported for analogous bonds in aminomethylphosphonic acid [Janicki & Starynowicz, 2010; 0.282 (8) and 0.193 (7) e Å^{-3} in the latter compound]. The P—O2 and P—O3 bonds, *i.e.* bonds with unprotonated O atoms, show a smaller excess density than the corresponding ones in the quoted compound [0.378 (10) and 0.333 (8) e Å^{-3}] – 0.07 e Å^{-3} less on average for both compounds.

The kinetic and potential energy densities at the BCPs, calculated from the electron-density distribution obtained from the multipole refinements and from the DFT calcula-

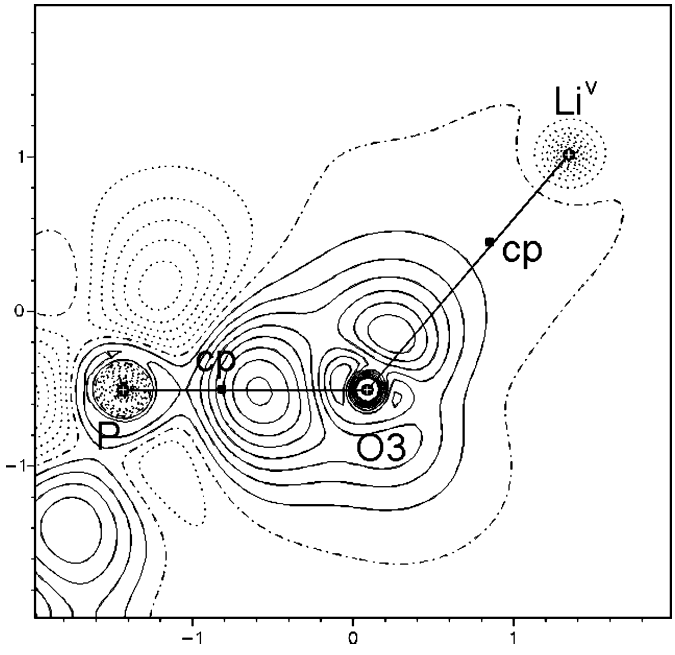

Figure 3
Static deformation density through the P—O3—Li^v plane. The contours are drawn every 0.05 e Å^{-3} (positive: solid, negative: dotted; zero: dashed–dotted); cp: critical point; the symmetry operator is taken from Table 4.

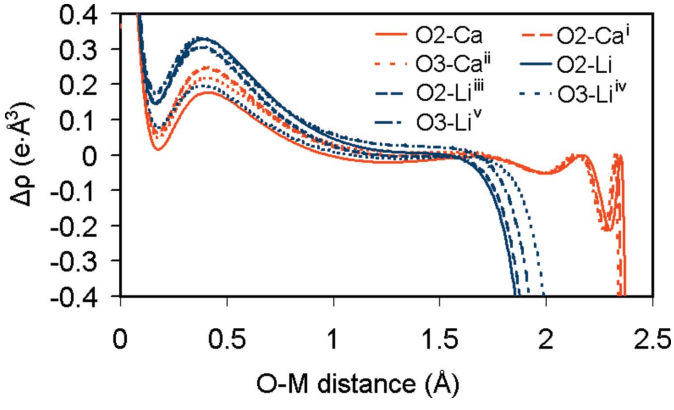

Figure 4
Diagram of compiled $\Delta\rho$ values along the O—Ca (red curves) and O—Li (blue curves) bonds. The symmetry operators are those from Table 4.

Table 5
Energy densities at the BCPs (in atomic units).

	Experimental				DFT			
	$G(r_c)$	$V(r_c)$	$E(r_c)$†	BD‡	$G(r_c)$	$V(r_c)$	$E(r_c)$†	BD‡
(I)								
P—O1	0.29	−0.43	−0.061	−0.71	0.33	−0.49	−0.16	−0.81
P—O2	0.40	−0.58	−0.18	−0.78	0.45	−0.64	−0.19	−0.83
P—O3	0.38	−0.55	−0.17	−0.78	0.44	−0.65	−0.21	−0.93
O1—H1	0.17	−0.79	−0.62	−1.84	0.07	−0.62	−0.54	−1.84
P—C	0.14	−0.31	−0.18	−0.98	0.09	−0.26	−0.18	−0.98
C—H2	0.19	−0.59	−0.40	−1.47	0.05	−0.35	−0.30	−1.09
C—H3	0.19	−0.57	−0.38	−1.43	0.05	−0.34	−0.29	−1.06
C—H4	0.19	−0.57	−0.38	−1.44	0.05	−0.34	−0.28	−1.04
O2—Ca	0.035	−0.028	0.007	0.27	0.036	−0.032	0.004	0.12
O2—Ca^{i}	0.038	−0.033	0.005	0.16	0.037	−0.033	0.005	0.15
O3—Ca^{ii}	0.039	−0.034	0.005	0.16	0.038	−0.033	0.005	0.15
H1—O3^{ii}	0.031	−0.061	−0.030	−0.46	0.041	−0.057	−0.016	−0.28
(II)								
P—O1	0.29	−0.43	−0.14	−0.70	0.33	−0.49	−0.16	−0.82
P—O2	0.42	−0.59	−0.17	−0.74	0.43	−0.62	−0.19	−0.86
P—O3	0.40	−0.57	−0.17	−0.71	0.46	−0.65	−0.19	−0.83
O1—H1	0.14	−0.71	−0.57	−1.78	0.08	−0.64	−0.56	−1.81
P—C	0.15	−0.32	−0.17	−0.95	0.09	−0.27	−0.18	−0.99
C—H2	0.21	−0.59	−0.39	−1.42	0.05	−0.33	−0.28	−1.05
C—H3	0.19	−0.56	−0.37	−1.41	0.05	−0.34	−0.29	−1.06
C—H4	0.20	−0.60	−0.39	−1.44	0.05	−0.34	−0.28	−1.05
O2—Li	0.046	−0.034	0.012	0.43	0.046	−0.038	0.008	0.26
O2—Li^{iii}	0.042	−0.030	0.012	0.52	0.043	−0.036	0.007	0.23
O3—Li^{iv}	0.028	−0.019	0.009	0.55	0.030	−0.024	0.006	0.27
O3—Li^{v}	0.037	−0.028	0.009	0.35	0.037	−0.030	0.007	0.27
H1—O3^{vi}	0.041	−0.044	−0.002	−0.06	0.039	−0.050	−0.011	−0.21

† $E(r_c) = G(r_c) + V(r_c)$. ‡ BD = $E(r_c)/\rho_c$; the symmetry codes are taken from Table 4.

tions, are presented in Table 5. The overall agreement is good, with the exception of bonds involving H atoms and P—C bonds, which is perhaps due to the general difficulty in studying the displacement parameters of H atoms.

As shown by Espinosa *et al.* (2002) analysis of $\nabla^2\rho_c$ combined with the bond-degree parameter, defined as $BD = E(r_c)/\rho_c$, where $E(r_c) = G(r_c) + V(r_c)$, allows a classification of bonds into pure closed-shell (CS; $\nabla^2\rho_c > 0$, $BD > 0$), shared-shell (S; $\nabla^2\rho_c < 0$, $BD < 0$) and transit closed-shell (TCS; $\nabla^2\rho_c > 0$, $BD < 0$) categories. In this paper we preserve the original terms given by these authors, although in our case the TCS type represents polarized covalent (shared-shell) interactions. In the S and TCS areas the BD parameters indicate the degree of covalency of the bond. Inspection of respective values for (I) and (II) reveals that all the C—H, P—C and O—H bonds belong to the S type of interactions – they are purely covalent with $\nabla^2\rho_c$ and $E(r_c)$ negative, whereas the P—O bonds are in the TCS region as indicated by positive values of the Laplacian and negative values of $E(r_c)$. This is consistent with the partially ionic character of P—O bonds as discussed elsewhere in this work. The parameters of metal–oxygen bonds for (I) and (II) locate these as CS interactions and it may be perhaps worth noting that bond degrees of the Ca—O bonds, both experimental and theoretical, are slightly lower than those for the Li—O bonds, *i.e.* they are shifted a little towards the covalency region. On the other hand, the hydrogen bonds seem to be in the TCS region.

It may be interesting to note that upon comparing the topological and BD parameters of the P—O(unprotonated) bonds to Mn—O ones reported by Marabello *et al.* (2004) for $KMnO_4$ it can be seen that both the classes have a somewhat similar nature, as both are in the TCS region, as shown by the reported experimental BD and Laplacian values for Mn—O bonds, −0.71 to −0.75 hartree e^{-1} and 27 (1)–28 (1) e Å^{-5}, whereas the experimental values for P—O bonds are in the range −0.71 to −0.789 hartree e^{-1} and 20.04 (4)–24.53 (3) e Å^{-5} for (I) and (II).

Ellipticities of the P—O and P—C bonds are generally close to 0, which means that there are no significant π interactions.

3.5. Theoretical calculations

In order to rationalize the results we have performed a series of DFT and then NBO calculations to obtain a deeper insight into the electronic structure of the anion and the metal–anion interactions. In particular it was interesting to check how the neighbourhood of the metal cations may modify the electron distribution in the hydrogen methylphosphonate. For this purpose we have performed the calculations separately for the $CH_3PO_3H^-$ anions with their geometries taken both from (I) (the anion with this geometry will be labelled as MPI) and (II) (MPII), and for the fragments containing the anion and bonded metal cations, *i.e.* $(CH_3PO_3H)Ca_3^{5+}$ (hereinafter $MPCa_3$) and $(CH_3PO_3H)Li_4^{3+}$ ($MPLi_4$).

It has been known that phosphorus compounds are hypervalent (Magnusson, 1990; Gilheany, 1994; Denehy *et al.*, 2007) and considerable hyperconjugation effects give rise to the fact that the overall electron arrangement is a combination of a number of component Lewis structures. A detailed analysis of the electron structure of the similar compound aminomethylphosphonic acid has been reported previously (Janicki & Starynowicz, 2010); the most important features will be discussed here.

In the NBO approach the orbitals obtained from SCF calculations may be transformed into a set of two centred bonding or antibonding orbitals and lone pairs. Such a transformation performed for (I) and (II) reveals that, as in the case of aminomethylphosphonic acid, all bonds within the MPI and MPII molecules are single. Scrutiny of the compositions and occupations of the natural bond orbitals within the CPO_3 stem in all the four systems (MPI, MPII, $MPCa_3$, $MPLi_4$; Table S3) leads to the following observations:

(i) comparison of MPI with $MPCa_3$ and MPII with $MPLi_4$ reveals that sharing of the O orbitals in σ(P—O) bonds increases if the O atom adjoins two metal cations [O2 in (I), O2 and O3 in (II)];

(ii) one of the lone pairs in each O atom is an sp^x hybrid with x ranging from 0.47 to 1.59, the remaining ones are of pure p type – similar hybridizations were calculated for O-atom lone pairs in aminomethylphosphonic acid;

(iii) in all four systems the occupancy of the sp^x hybrids is practically identical;

(iv) upon addition of the metal cations the occupancy of p lone pairs increases due to polarization, although in the case of O3 in $MPCa_3$ this growth is small;

(v) out of the four σ^*(P—O or P—C) orbitals a decrease in occupancy is distinct in the case of σ^*(P—O1) and σ^*(P—C) in both $MPCa_3$ and $MPLi_4$.

As was indicated by Denehy *et al.* (2007) hyperconjugation results in non-zero occupancy of some antibonding orbitals at the cost of reduction of occupancy of bonding orbitals or lone pairs interacting with the former ones. Smaller occupancies of antibonding orbitals in $MPCa_3$ and $MPLi_4$ in comparison with MPI and MPII mean that the hyperconjugation is partially quenched in the presence of metal cations in the vicinity of the O atoms. This fact may be demonstrated by calculating shares of possible resonance Lewis structures in the overall wavefunctions of the studied systems. The electronic structures of MPI and MPII may be described as combinations of seven resonance structures. These structures may be merged into four if equivalence of O2 and O3 is assumed. These forms have comparable shares in the case of uncoordinated methylphosphonate anions; see Fig. 5 for the constitution of these forms together with their resonance weights. The share of the basic one, $CH_3—P^+—OH(—O^-)_2$ [form (I) in Fig. 5] is 14.1% in MPI and 22.1% in MPII. In $MPCa_3$ and $MPLi_4$ the share of this form grows to 62.8 and 65.8%. The other forms represent structures with broken P—O or P—C bonds, such as $H_3C—P^+(OH^-)(—O^-)(=O)$ (II), $H_3C^-P^+—OH(—O^-)(=O)$ (III) or $H_3C—P^+—OH(=O)(O^{2-})$ (IV). They practically disappear upon coordination of the metal cations. Detailed calculations show that in more practical terms this means growth of ρ_c of the P—C and P—OH bonds (increases of 0.03 and 0.04–0.05 e Å^{-3}), accompanied by 0.01–0.02 e Å^{-3} drops at the critical points of P—O2 and P—O3 bonds. However, it must be noted that the model calculations presented here do not include hydrogen bonds which may further modify the results. Nevertheless, the above predictions seem to be in good accordance with the experimental results – in comparison with the data presented for aminomethylphosphonic acid, where the hyperconjugation plays a greater role, the experimental ρ_c values for the P—C bond in (I) and (II) are 0.05 e Å^{-3} larger, and for the P—O ones – 0.04–0.10 e Å^{-3} smaller. The values of ρ_c for the P—O(H) bonds in the present compounds are approximately 0.02 e Å^{-3} smaller than in aminomethylphosphonic acid, contrary to the effect expected from considering the hyperconjugation alone. This may be brought about by two reasons: various hydrogen bonding in the compounds compared and/or somewhat imperfect modelling of the charge density around the hydroxyl H atoms, as mentioned earlier.

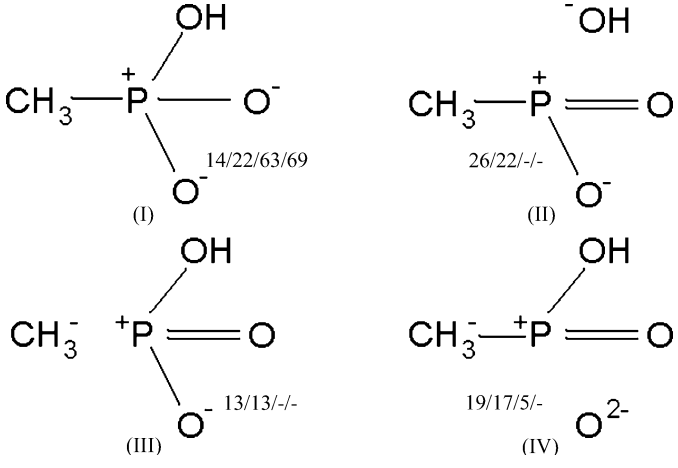

Figure 5
The basic Lewis forms together with their resonance weights (%) in the following order: MPI/MPII/$MPCa_3$/$MPLi_4$. For the sake of simplicity O2 and O3 are not distinguished. The shares below 5% are omitted.

4. Conclusions

The topology of experimental and theoretical electron-density distributions for two new crystal structures, calcium bis(hydrogen methylphosphonate) (I) and lithium hydrogen methylphosphonate (II), has been analyzed. The two approaches are in satisfactory agreement.

Examination of the bond properties reveals the covalent nature of C—H, P—C and O—H bonds, whereas the P—O bonds show partially closed-shell interactions, which is consistent with their partially ionic character. As in other phosphonates, there is a difference between the protonated and unprotonated O atoms; the latter accumulate more negative charge. Also the electron densities at the BCP of the P—O(H) bonds are smaller than at the P—O bonds.

A closer inspection reveals only small changes in the electronic structure of the anions upon coordination to the cations. Owing to the neighbourhood of metal cations hyperconjugation effects are quenched, which is manifested by a small growth of the P—C BCP density accompanied by a small decrease in the density at the P—O2 and P—O3 BCPs, compared with analogous values in aminomethylphosphonic acid. Marginal polarization effects may be observed in the case of the Li compound, where they are visible in the deformation densities of the Li—O bonds. Both the Laplacian and bond degree values confirm that the Li—O bonds are more ionic than the Ca—O ones.

The authors wish to thank Professor T. Lis for the data collection and valuable discussion. The *ADF* calculations have been carried out at the Wrocław Centre for Networking and Supercomputing (http://www.wcss.wroc.pl), grant No. 58.

References

Abramov, Yu. A. (1997). *Acta Cryst.* A**53**, 264–272.
Alberti, G. (1996). *Adv. Mater.* **8**, 291–303.
Allen, F. A., Kennard, O. & Watson, D. G. (1987). *J. Chem. Soc. Perkin Trans. II*, pp. S1–S19.
Aubert, E., Porcher, F., Souhassou, M. & Lecomte, C. (2003). *Acta Cryst.* B**59**, 687–700.
Bader, R. F. W. (1994). *Atoms in Molecules: A Quantum Theory*. Oxford University Press.
Baerends, E. J. *et al.* (2008). *ADF*2008.01. SCM, Theoretical Chemistry, Vrije Universiteit, Amsterdam, The Netherlands, http://www.scm.com.
Bianchi, R., Gatti, C., Adovasio, V. & Nardelli, M. (1996). *Acta Cryst.* B**52**, 471–478.
Blessing, R. H. (1987). *Crystallogr. Rev.* **1**, 3–58.
Cao, G., Lynch, V. M., Swinnea, J. S. & Mallouk, T. E. (1990). *Inorg. Chem.* **29**, 2112–2117.
Cheng, C.-Y. & Lin, K.-J. (2006). *Acta Cryst.* C**62**, m363–m365.
Clark, R. C. & Reid, J. S. (1995). *Acta Cryst.* A**51**, 887–897.
Clementi, E. & Roetti, C. (1974). *At. Data Nucl. Data Tables*, **14**, 177–478.
De Clercq, E. & Holý, A. (2005). *Nature*, **4**, 928–940.
Denehy, E., White, J. M. & Williams, S. J. (2007). *Inorg. Chem.* **46**, 8871–8886.
Du, Z.-Y., Sun, Y.-H., Xu, X., Xu, G.-H. & Xie, Y.-R. (2010). *Eur. J. Inorg. Chem.* pp. 4865–4869.
Espinosa, E., Alkorta, I., Elguero, J. & Molins, E. (2002). *J. Chem. Phys.* **117**, 5529–5542.
Espinosa, E., Lecomte, C. & Molins, E. (1999). *Chem. Phys. Lett.* **300**, 745–748.
Espinosa, E., Lecomte, C., Molins, E., Veintemillas, S., Cousson, A. & Paulus, W. (1996). *Acta Cryst.* B**52**, 519–534.
Espinosa, E., Molins, E. & Lecomte, C. (1998). *Chem. Phys. Lett.* **285**, 170–173.
Espinosa, E., Souhassou, M., Lachekar, H. & Lecomte, C. (1999). *Acta Cryst.* B**55**, 563–572.
Gilheany, D. G. (1994). *Chem. Rev.* **94**, 1339–1374.
Glendening, E. D., Badenhoop, J. K., Reed, A. E., Carpenter, J. E., Bohmann, J. A., Morales, C. M. & Weinhold, F. (2001). *NBO*5.0. Theoretical Chemistry Institute, University of Wisconsin, Madison, USA.
Gliga, A., Klare, H., Schumacher, M., Soki, F., Neudoerfl, J. M. & Goldfuss, B. (2011). *Eur. J. Org. Chem.* pp. 256–263.
Hansen, N. K. & Coppens, P. (1978). *Acta Cryst.* A**34**, 909–921.
Hirshfeld, F. L. (1976). *Acta Cryst.* A**32**, 239–244.
Hirshfeld, F. L. (1977). *Theor. Chim. Acta*, **44**, 129–138.
Ichikawa, M., Gustafsson, T. & Olovsson, I. (1998). *Acta Cryst.* B**54**, 29–34.
Janicki, R. & Starynowicz, P. (2010). *Acta Cryst.* B**66**, 559–567.
Jauch, W. & Reehuis, M. (2005). *Acta Cryst.* A**61**, 411–417.
Langley, K. J., Squattrito, P. J., Adani, F. & Montoneri, E. (1996). *Inorg. Chim. Acta*, **253**, 77–85.
Lyssenko, K. A., Grintselev-Knyazev, G. V. & Antipin, M. Yu. (2002). *Mendeleev Commun.* pp. 128–130.
Madsen, A. Ø. (2006). *J. Appl. Cryst.* **39**, 757–758.
Magnusson, E. (1990). *J. Am. Chem. Soc.* **112**, 7940–7951.
Marabello, D., Bianchi, R., Gervasio, G. & Cargnoni, F. (2004). *Acta Cryst.* A**60**, 494–501.
Matczak-Jon, E. & Videnova-Adrabińska, V. (2005). *Coord. Chem. Rev.* **249**, 2458–2488.
Melegari, M., Suman, M., Pirondini, L., Moiani, D., Massera, C., Ugozzoli, F., Kalenius, E., Vainiotalo, P., Mulatier, J.-C., Dutasta, J.-P. & Dalcanale, E. (2008). *Chem. Eur. J.* **14**, 5772–5779.
Murphy, P. J. (2004). *Organophosphorus Reagents*. Oxford University Press.
Ortiz, J. C. & Bo, C. (1998). *Xaim*. Universitat Rovira i Virgili, Tarragona, Spain.
Oxford Diffraction (2010). *CrysAlis CCD*, Version 1.171.33.32. Oxford Diffraction Ltd, Yarnton, UK.
Perdew, J. P., Chevary, J. A., Vosko, S. H., Jackson, K. A., Pederson, M. R., Singh, D. J. & Fiolhais, C. (1992). *Phys. Rev. B*, **46**, 6671–6687.
Pérès, N., Boukhris, A., Souhassou, M., Gavoille, G. & Lecomte, C. (1999). *Acta Cryst.* A**55**, 1038–1048.
Rao, K. P. & Vidyasagar, K. (2005). *Eur. J. Inorg. Chem.* pp. 4936–4943.
Rodrigues, B. L., Tellgren, R. & Fernandes, N. G. (2001). *Acta Cryst.* B**57**, 353–358.
Savigniac, P. & Iorga, B. (2003). *Modern Phosphonate Chemistry*. Boca Raton, FL: CRC Press LLC.
Sheldrick, G. M. (2008). *Acta Cryst.* A**64**, 112–122.
Ślepokura, K. & Lis, T. (2003). *Acta Cryst.* C**59**, m76–m78.
Slouf, M., Holy, A., Petříček, V. & Cisarova, I. (2002). *Acta Cryst.* B**58**, 519–529.
Souhassou, M., Espinosa, E., Lecomte, C. & Blessing, R. H. (1995). *Acta Cryst.* B**51**, 661–668.
Sparidans, R. W., Twiss, I. M. & Talbot, S. (1998). *Pharm. World Sci.* **20**, 206–213.
Stone, J. W., Smith, M. D. & zur Loye, H.-C. (2007). *J. Chem. Crystallogr.* **37**, 103–108.
Thompson, M. E. (1994). *Chem. Mater.* **6**, 1168–1175.
Volkov, A., Macchi, P., Farrugia, L. J., Gatti, C., Mallinson, P., Richter, T. & Koritsánszky, T. (2006). *XD*2006. University of New York at Buffalo, NY, USA.
Walawalkar, M. G., Murugavel, R., Voigt, A., Roesky, H. W. & Schmidt, H.-G. (1997). *J. Am. Chem. Soc.* **119**, 4656–4661.
Westheimer, F. H. (1987). *Science*, **235**, 1173–1178.
Zeng, R., Xiangkai, F. & Chengbin, G. (2006). *J. Mater. Sci.* **41**, 4771–4776.
Zhang, Y. & Clearfield, A. (1992). *Inorg. Chem.* **31**, 2821–2826.
Zhang, Y., Scott, K. J. & Clearfield, A. (1993). *Chem. Mater.* **5**, 495–499.
Zhurova, E. A. & Tsirelson, V. G. (2002). *Acta Cryst.* B**58**, 567–575.